

## Pedestal-to-Wall 3D Fluid Transport Simulations on DIII-D and NSTX

J.D. Lore<sup>a</sup>, J-W. Ahn<sup>a</sup>, A.R. Briesemeister<sup>a</sup>, J.M. Canik<sup>a</sup>, N.M. Ferraro<sup>b</sup>, H. Frerichs<sup>c</sup>, A. McLean<sup>d</sup>, J-K. Park<sup>b</sup>, M.W. Shafer<sup>a</sup>, R.S. Wilcox<sup>a</sup>

<sup>a</sup> Oak Ridge National Laboratory, Oak Ridge, TN, USA.

<sup>b</sup> Princeton Plasma Physics Laboratory, Princeton, NJ, USA.

<sup>c</sup> University of Wisconsin-Madison, Madison, WI, USA.

<sup>d</sup> Lawrence Livermore National Laboratory, Livermore, CA, USA.

email: lorejd@ornl.gov

The 3D edge transport code EMC3-EIRENE [1] is used to test magnetic field models with and without plasma response against pedestal, edge, and divertor diagnostic data on the DIII-D and NSTX experiments. None of the models tested can reproduce the measured ‘lobe’ structure in the scrape off layer (SOL) temperature and density while maintaining the experimental pedestal pressure gradient. A validated 3D ‘pedestal-to-wall’ simulation capability is required to make predictions for ITER, as intrinsic and applied 3D magnetic fields can affect pedestal transport and stability and cause toroidally and poloidally localized fluxes and non-axisymmetric erosion of plasma facing components. The magnetic fields used in the EMC3-EIRENE calculations include axisymmetric equilibria (EFIT [2]), a superposition of EFIT and 3D vacuum perturbation fields (‘vacuum approximation’), and 3D MHD codes which include plasma response (VMEC [3], IPEC/GPEC [4], M3D-C1 [5]). The EMC3-EIRENE and plasma response calculations are tested by identifying configurations for which the magnetic field models produce measureable differences in the transport simulations and constraining the code inputs using experimental data.

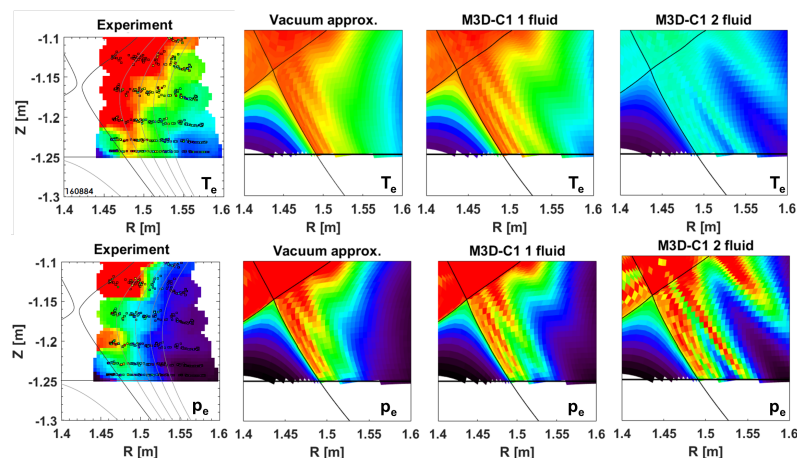


**Fig. 1. Electron temperature (upper) and pressure (lower) contours from DTS measurements and EMC3-EIRENE simulations for 3 magnetic field calculations.**

The DIII-D divertor Thomson scattering (DTS) system shows significant structure in the scrape off layer that is not present in plasmas without applied perturbations. Figure 1 shows contours of the electron temperature (upper left panel) and pressure (lower left panel) as measured by the during a x-point sweep for an H-mode plasma with magnetic perturbations applied using the I-coils with odd-parity. In this configuration the radial magnetic field is dominantly non-resonant, leading to relatively small magnetic lobes in the vacuum approximation as compared to an even-parity perturbation of similar amplitude. Note that ELM suppression experiments are typically performed with even-parity perturbations, but this comparison using odd-parity was selected because it produced a significant difference in the calculated magnetic field structure between vacuum and two fluid models. This can be seen by comparing the EMC3-EIRENE calculations using the magnetic field from linearized single-fluid and two-fluid M3D-C1 simulations (3<sup>rd</sup> and 4<sup>th</sup> column). The two-fluid cases

show an extended lobe structure with high  $T_e$  that extends to the divertor plate, which is not reflected in the DTS data. The single-fluid calculations, on the other hand, are similar in structure to the vacuum fields (1st column). The two-fluid simulations contain terms with large uncertainties in the open field line region (e.g., rotation profile) that will be constrained against the experimental data using the EMC3-EIRENE simulation. These simulations can be performed much more rapidly than non-linear M3D-C1 calculations while including additional effects such as interaction with neutral particles.

The DTS measurements are only one important aspect of a full pedestal-to-wall edge transport validation process. The magnetic field and transport models must be able to simultaneously reproduce the edge structure and the measured pressure gradient in the pedestal to make a comprehensive prediction for ITER. Magnetic field models with a strong resonant response that produces significant stochasticity cannot support the experimental pressure gradient in the pedestal in EMC3-EIRENE simulations, even for an extremely small value of (prescribed) cross-field diffusivity. In the odd-parity case above, the two-fluid simulations result in a pedestal pressure gradient four times smaller than the vacuum or single-fluid cases. Simulations for even-parity perturbations, on the other hand, have yielded larger pedestal pressure gradients when using M3D-C1 two-fluid fields as compared to the vacuum perturbation. In these latter cases the plasma response results in a reduction in resonant radial magnetic field and a lower level of stochasticity. Validation of the plasma transport model is also underway, indicating the importance of kinetic corrections (not included in EMC3) which are shown in 2D edge calculations to increase the simulated pedestal pressure.

The application of 3D fields can also affect the transition to detachment. NSTX experiments showed that 3D fields could cause a detached plasma to reattach [6]. At large major radius the additional heat flux peaks from strike point splitting remained present even at high density. Increasing the density further caused a drop in confinement. EMC3-EIRENE simulations of NSTX experiments reproduced the experimental trends, with the primary heat flux peak reduced before the outer lobes detach (Fig. 2). At the highest density shown in Fig. 2 an axisymmetric simulation is detached.

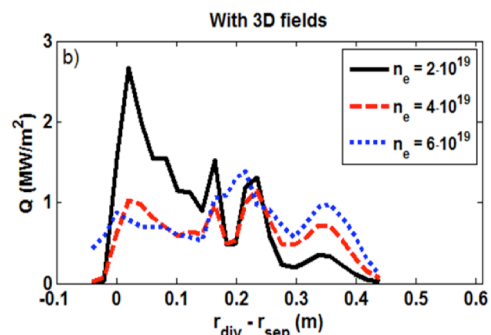


Fig 2. EMC3-EIRENE simulation of NSTX plasma with 3D perturbations showing heat flux at outer lobes at high density.

In summary, 3D pedestal to wall simulations including plasma response are tested against DIII-D and NSTX experimental data. None of the magnetic field models used (with and without plasma response) can reproduce the edge and pedestal measurements. Qualitative trends, such as the effect of 3D fields on detachment are captured. Work supported by the US DOE under DE-AC05-00OR22725<sup>a</sup>, DE-AC02-09CH11466<sup>b</sup>, DE-SC0012315<sup>c</sup>, DE-SC0013911<sup>c</sup>, DE-AC52-07NA27344<sup>d</sup>, and DE-FC02-04ER54698.

- [1] Y. Feng, et al., J. Nucl. Mater., 241-243, 930 (1997)
- [2] L.U. Lao, et al., Nucl. Fusion 30 1035 (1990).
- [3] S.P. Hirshman, and J.C. Whitson, Phys. Fluids 26, 3353 (1983).
- [4] J.-K. Park, et al., Phys. Plasmas 14 052110 (2007).
- [5] S. Jardin, et al., J. Phys. Conf. Series 125 012044 (2008).
- [6] J.-W. Ahn, et al., PPCF 56 015005 (2014).